



HAL
open science

Effect of glucose-induced Maillard reaction on physical, structural and antioxidant properties of chitosan derivatives-based films

Sawsan Affes, Rim Nasri, S.M. Li, Thierry Thami, Arie van Der Lee, Moncef Nasri, Hana Maalej

► To cite this version:

Sawsan Affes, Rim Nasri, S.M. Li, Thierry Thami, Arie van Der Lee, et al.. Effect of glucose-induced Maillard reaction on physical, structural and antioxidant properties of chitosan derivatives-based films. Carbohydrate Polymers, 2021, 255, pp.117341. 10.1016/j.carbpol.2020.117341 . hal-03359461

HAL Id: hal-03359461

<https://hal.umontpellier.fr/hal-03359461v1>

Submitted on 30 Sep 2021

HAL is a multi-disciplinary open access archive for the deposit and dissemination of scientific research documents, whether they are published or not. The documents may come from teaching and research institutions in France or abroad, or from public or private research centers.

L'archive ouverte pluridisciplinaire **HAL**, est destinée au dépôt et à la diffusion de documents scientifiques de niveau recherche, publiés ou non, émanant des établissements d'enseignement et de recherche français ou étrangers, des laboratoires publics ou privés.

Highlights

- Films with varying Mw chitosan and CDP were prepared and heat-treated;
- Functional and structural properties of films were modified by thermal treatment;
- Antioxidant activities of the films were improved due to MR products development.

25 **Abstract**

26 This work focused on studying the physicochemical and antioxidant properties changes
27 of varying molecular weight (Mw) chitosan-depolymerization products (CDP)-based films
28 occurring after crosslinking by heat-treatment and Maillard reaction (MR). Based on color
29 properties and browning index, an enhancement of films properties was observed after
30 treatment at 90 °C with a reduction in their water content, solubility and contact angle. Brown
31 MR products were developed in heated films containing glucose thus improving their barrier
32 properties. This effect was more pronounced in lower Mw-CDP based films. In addition,
33 according to TGA, EAB and TS analyses an improvement in heat-treated films thermal stability
34 and mechanical properties was detected and further confirmed through FTIR, X-ray and SEM
35 analyses. The evaluation of the antioxidant potential through four different assays allowed to
36 conclude that glucose addition, thermal treatment and the use of low Mw-CDP highly enhanced
37 the MR-modified films antioxidant capacity. Consequently, MR crosslinked chitosan-based
38 films could be potentially used as an alternative for bioactive and functional packaging effective
39 in food oxidation inhibition, especially using low Mw chitosan derivatives.

40 **Keywords:** Chitosan-depolymerization products, Molecular weight, Films, Maillard reaction,
41 Physicochemical characterization, Antioxidant potential.

42

43

44

45

46

47

48 **1. Introduction**

49 Increasing environmental concerns led to a growing interest on research and development
50 of biodegradable films based on renewable resources as alternative to synthetic packaging
51 traditionally used in biomedical and food industries (Fernández-de Castro et al., 2016; Ruban
52 et al., 2009). For this purpose, biopolymers, including proteins and polysaccharides are
53 increasingly being used to prepare composite films and coating (Etxabide, Urdanpilleta,
54 Gómez-Arriaran, de la Caba, & Guerrero, 2017; Kchaou, Benbettaieb, Jridi, Nasri, &
55 Debeaufort, 2019). Among the most studied biopolymers, chitosan, a natural polysaccharide
56 derived from chitin and composed of D-glucosamine and N-acetylglucosamine units, deserves
57 special attention due its biological properties, such as biocompatibility, non-toxicity,
58 biodegradability and good film-forming ability (Affes et al., 2020a; Hajji, Younes, Affes,
59 Boufi, & Nasri, 2018). Such characteristics of chitosan depended on its acetylation degree,
60 distribution of acetyl groups, viscosity and especially its molecular weight (Mw). Chitosan
61 derivatives with attractive characteristics, such as low Mw, reduced viscosity and improved
62 antioxidant and antimicrobial potentials, were produced through depolymerization of chitosan
63 by physical, chemical or enzymatic hydrolysis methods (Affes et al., 2019; Aljbour, Beg, &
64 Gimbun, 2019; Sun et al., 2017).

65 Some studies have been made to characterize chitosan or chitosan depolymerization
66 products (CDP)-based films as alternative to protect food from drying and oxidation
67 (Fernández-de Castro et al., 2016). In this context, chitosan or CDP-based films properties,
68 such as water resistance, can be improved by enzymatic, chemical and physical modifications
69 to extend their application fields (Leceta, Guerrero, Ibarburu, Dueñas, & de la Caba, 2013b).
70 There are not many reports concerning non-enzymatic cross-linking methods of chitosan
71 films. As two kinds of different cross-linking browning methods, caramelisation is caused by
72 direct heating of carbohydrate, while Maillard reaction (MR) refers to the condensation

73 reactions between nitrogen-containing compounds and carbonyl group of reducing sugars (Li,
74 Lin, & Chen, 2014). Subsequently, heat treatment is a physical method that had a noticeable
75 effect on improvement of film properties, especially water solubility, thermal stability and
76 mechanical and barrier properties (Fernández-de Castro et al., 2016; Leceta et al., 2013b;
77 Rivero, Garía, & Pinotti, 2012). Whereas, crosslinking through MR is a chemical process
78 involving three stages in which the initial products are called shift bases that form Amadori
79 products via rearrangement, which undergo further reactions to form irreversible advanced
80 glycation end products (Etxabide et al., 2017; Sun et al., 2017). This method generates
81 fluorescent, brown MR products able to improve chemical, sensory, antioxidant and
82 antimicrobial activities of chitosan films. To control the extension of MR, in order to obtain
83 the properties required for a specific application, various factor should be analyzed, including
84 temperature, time, pH, water activity and concentration, type and ratio of used carbonyl group
85 compounds and reducing sugar (Gullón et al., 2016).

86 The purpose of this work was to study changes undergone, by crosslinking and Maillard
87 reaction development, in varying Mw chitosan or CDP-based films by monitoring their
88 physical, functional and microstructural properties before and after heat-treatment at 90 °C
89 and with and without glucose addition.

90 **2. Materials and methods**

91 **2.1. Materials**

92 Chitosan (Ch) was prepared from shrimp shells chitin and hydrolyzed using the
93 chitosanolytic preparation from *Bacillus licheniformis* strain as described in our previous study
94 (Affes et al., 2020b). After incubation of the chitosan solution at 50 °C in the presence of the
95 chitosanolytic preparation, samples were withdrawn at 1 and 24 h, heated at 100 °C for 10 min,
96 neutralized to pH 8.0 and centrifuged for 30 min at 8,000 x g. The insoluble part at 1 and 24 h
97 were freeze-dried and referred as chitosan depolymerization products (CDP) C1 and C24,

98 respectively. The average molecular weight (Mw), the intrinsic viscosity, the acetylation degree
99 and the crystallinity index of Ch, C1 and C24 were determined by SEC-HPLC, a semi-
100 automatic Ubbelohde viscometer, the first derivative UV-spectrophotometric method and using
101 on an X'Pert SW X-ray diffractometer (Philips), respectively.

102 Chitosan, C1 and C24 were employed as biopolymers for films preparation. D (+)
103 anhydrous-glucose (Glu) ($C_6H_{12}O_6$; 180 g mol^{-1}) was used as reducing sugars to initiate the
104 Maillard reaction (MR) in chitosan-based films. Anhydrous glycerol was purchased from Fluka
105 (98% purity, Fluka Chemical, Germany) and used as plasticizer for the films. All other reagents
106 were of analytic grade.

107 **2.2. Films preparation**

108 Chitosan or CDP-based films were prepared according to the casting technique. A mother
109 film-forming solution (FFS) was firstly prepared by dissolving the used polymer (10 mg/ml) in
110 acetic acid (1%, v/v) and stirred continuously at room temperature to obtain homogeneous
111 solution. Then, two films categories were prepared. First, chitosan or CDP-based films were
112 obtained by adding glycerol to the FFS, at a concentration of 15% (w/w polymer), and stirring
113 for 30 min. Second, polymer-glucose-containing films were prepared to promote MR
114 development. Glucose (0.5 mg/ml) was added to the FFSs containing 15% (w/w polymer) of
115 glycerol. Subsequently, a volume of 34.0 ml of each mixture with or without glucose was cast
116 in Petri dishes (13.5 x 13.5 cm) and left to dry for 48 h at 25 °C, until the total evaporation of
117 the solvent.

118 After peeling, a first half of all films, referred as F1, F2 and F3 (using chitosan, C1 and
119 C24, respectively) for films without glucose and F1-Glu, F2-Glu and F3-Glu for films
120 containing glucose, were considered as controls. Then to favour MR, the second half of all the
121 films was heated in an oven at $90 \pm 2 \text{ °C}$ for 24 h. Heated films without glucose were named
122 F1-90, F2-90 and F3-90, while, heated films containing glucose were referred as F1-Glu-90,

123 F2-Glu-90 and F3-Glu-90. All prepared films were then conditioned at 25 °C and 50% relative
124 humidity (RH) before analyses, except for FTIR, XRD, TGA and DSC measurements, films
125 were equilibrated at 0% RH.

126 **2.3. Physical and structural characterization of the prepared films**

127 **2.3.1. Color properties and browning index**

128 Color of the films was performed using a CR-5 colorimeter Konica Minolta (Sensing
129 Europe B.V) and recorded using the color parameters CIE L* a* and b*. L* was expressed as
130 lightness/brightness, a* is a measure of greenness/redness and b* was expressed as
131 blueness/yellowness values. The total color changes (ΔE_1^* and ΔE_2^*) of the blend films were
132 calculated according to the following equation:

$$133 \quad \Delta E = \sqrt{((L^* - L_0^*)^2 + (a^* - a_0^*)^2 + (b^* - b_0^*)^2)} \quad \text{Eq (1)}$$

134 where L_0^* , a_0^* , b_0^* are the colorimetric parameters of the standard (ΔE_1^* was measured using
135 the film F1 as standard, while, ΔE_2^* was calculated using the parameters of each control film
136 F1, F2 and F3 as standard in the different Mw-chitosan based films) and L*, a*, b* are the
137 values of the tested films.

138 The obtained CIE Lab values were then used to calculate the browning index (BI) as
139 mentionned in equation 2:

$$140 \quad BI = \frac{100 \times (z - 0.31)}{0.172} \quad \text{with} \quad z = \frac{a^* + 1.75 (L^*)}{5.645 (L^*) + (a^*) - 3.012 (b^*)} \quad \text{Eq (2)}$$

141 **2.3.2. Ultraviolet-visible barrier**

142 Ultraviolet-visible (UV-Vis) spectroscopy of the films was performed by using an UV-
143 vis recording spectrophotometer (Shimadzu UV-2401PC) in the wavelength range from 200
144 to 800 nm. The films were cut into rectangle (1.0 x 3.0 cm) and placed in the test cell of the
145 spectrophotometer. An empty test cell was used as a reference.

146 **2.3.3. Water content and solubility**

147 To determine the moisture content (WC) of the films (g_{moisture}/100 g_{film}), 100 mg of each
148 film sample were dried in an oven at 105 °C until constant weight was reached. The weights
149 before and after drying were measured and the water content was calculated as follows:

$$150 \quad \text{WC (\%)} = \frac{(m_i - m_f)}{m_i} \times 100 \quad \text{Eq (3)}$$

151 where m_i and m_f are the initial and the final film weight (g), respectively. Three replicates for
152 each film were performed.

153 The water solubility of the films was determined according to the Gennadios, Handa,
154 Froning, Weller, & Hanna (1998) method. Film samples (2.0 x 5.0 cm) were weighted and
155 transferred to centrifuge tube containing 30 ml of distilled water with 0.1% (w/v) sodium azide
156 as antimicrobial agent. The mixture was shaken at 200 rpm speed at 25 °C during 24 h and then
157 centrifuged at 8000 rpm at 25 °C for 10 min. The undissolved debris were dried at 105 °C for
158 24 h to determine the remaining pieces of films. Water solubility (WS) was calculated according
159 to the following equation:

$$160 \quad \text{WS (\%)} = \frac{[(m_i \times (100 - \text{WC})) - m_f]}{(m_i \times (100 - \text{WC}))} \times 100 \quad \text{Eq (4)}$$

161 where m_i and m_f are the initial and final film weights (g), respectively and WC is the water
162 content of each film sample (%).

163 **2.3.4. Water contact angle**

164 The contact angle measurements were carried out using the sessile drop method on a
165 goniometer (Drop Shape Analyzer 30 from Kruss GmbH), equipped with an image analysis
166 software (ADVANCE). First, films were fixed in a glass plate. Then, a droplet of water (3 µl)
167 was deposited on the film surface with a precision syringe. The method is based on image
168 processing and curve fitting for contact angle measurement from a theoretical meridian drop
169 profile, determining contact angle between the baseline of the drop and the tangent at the drop
170 boundary. Six measurements per films were carried out. All the tests were conducted in an

171 environmental chamber with a constant environment at a temperature of 25 (\pm 2) °C and a
172 relative humidity of 50 (\pm 1) %.

173 **2.3.5. Films thickness**

174 The thickness of the prepared films was measured using a micrometer (Digimatic IP65,
175 Mitutoyo, France). Six random locations around each film sample were used for average
176 thickness determination. The mean value was considered for mechanical properties parameters
177 calculation.

178 **2.3.6. Films mechanical properties**

179 The films mechanical properties were performed based on the determination of the tensile
180 strength (TS, MPa) and elongation at break (EAB, %) parameters by using a rheometer
181 apparatus (Physica MCR, Anton Paar, GmbH, France) equipped with a mechanical property
182 measuring geometry. Prior to analysis, all the film samples were equilibrated at 25 °C and 50%
183 RH for a week and their thickness was measured. Then, rectangular films (1.0 x 4.5 cm) were
184 cut to get tensile test piece with an accurate width and parallel sides throughout the entire length.
185 Based on the ISO standard, equilibrated films samples, retained in the extension grips of the
186 measuring system, were subjected to a uniaxial tensile test, with a deformation rate of 5 mm/min
187 until breaking. Rheoplus software was used for the estimation of TS and EAB, corresponding
188 respectively to the maximum load and the final extension at break from the stress-strain curves.
189 Measurements were carried out at 25 °C and six samples for each formulation were tested.

190 **2.3.7. Thermal stability analysis**

191 The thermal stability of the film samples was carried out using a thermogravimetric
192 analysis (TGA, Q500 High Resolution, TA Instruments). This technique allows the continuous
193 weighting of the film sample mass in percentage (%) as a function of the temperature rise in a
194 controlled nitrogen atmosphere. The film samples were heated from 30 to 600 °C at a heating

195 rate of 20 °C/min. Weight loss (Δw , %), temperature of maximum degradation (T_{max} , °C) and
196 final residue at 600 °C (%) values were determined using TA Universal Analysis 2000 software
197 (Version 4.5 A, TA instruments).

198 **2.3.8. Fourier transform infrared spectroscopy (FTIR) analysis**

199 The FTIR spectra of film samples were determined using a spectrometer (Agilent
200 Technologies, Cary 630 series) equipped with an attenuated reflection accessory (ATR)
201 containing a diamond/ZnSe crystal, at 25 °C. 32 scans were collected with 4 cm^{-1} resolution
202 in 500-4000 cm^{-1} wavelength range. Prior to analysis, calibration was performed using
203 background spectrum recorded from the clean and empty diamond. Data analysis and
204 treatment were carried out by using the OMNIC spectra software (Thermo Fisher Scientific).

205 **2.3.9. X-ray diffraction (XRD) analysis**

206 XRD analysis of the prepared films was carried out on a Philips diffractometer using a
207 Cu K_α radiation source. The samples were scanned continuously at a voltage of 40 kV and a
208 current of 30 mA with the ranging 2θ from 7 to 40 °. Where θ is the incidence angle of the X-
209 ray beam on the sample.

210 **2.3.10. Films microstructure**

211 The surface and cross-section morphology of the films were assessed using a scanning
212 electron microscopy (SEM, Hitachi S4800). The cross-section observations were performed at
213 an angle of 90 ° to the surface and using different magnifications. Prior to imaging, samples
214 were cryo-fractured by immersion in liquid nitrogen, cut and fixed on the SEM support using
215 double side adhesive tape under an accelerating voltage of 2 kV and an absolute pressure of 60
216 Pa, after sputter coating with a 5 nm thick gold.

217 **2.4. Films antioxidant potential**

218 **2.4.1. ABTS⁺ radical-scavenging activity**

219 The ABTS⁺ radical-scavenging capacity of the films was determined according to the
220 method of Re et al. (1999). This test is based on the ability of antioxidant molecules to quench
221 the long-lived ABTS⁺ species. The ABTS⁺ radical was generated by mixing 7 mM ABTS⁺
222 solution with 2.45 mM potassium per sulphate. This solution was then diluted with ethanol to
223 adjust the absorbance to approximately 0.7 at 734 nm. 100 µl of distilled water containing 10
224 mg film samples were added to 900 µl of diluted ABTS⁺ solution. A solution without samples
225 was recorded as control. The mixtures were incubated at 25 °C for 10 min. The absorbance was
226 then determined at 734 nm and ABTS⁺ radical-scavenging capacity was computed using the
227 following equation:

$$228 \quad \text{ABTS}^+ \text{ radical scavenging activity (\%)} = \frac{A_C + A_B - A_R}{A_C} \times 100 \quad \text{Eq (5)}$$

229 where A_C is the absorbance of the control ABTS⁺ solution; A_R is the absorbance of film sample
230 with ABTS⁺ solution and A_B is the absorbance of blank tubes containing sample without
231 addition of ABTS⁺ solution. The values are presented as the means of triplicate analyses.

232 **2.4.2. DPPH radical-scavenging assay**

233 The ability of the elaborated films to scavenge DPPH radical was determined according
234 to Bersuder, Hole, & Smith (1998). Firstly, the films were cut into small pieces (m = 10 mg)
235 and immersed in 500 µl of disillited water. 500 µl of each film sample were added to 375 µl of
236 99.5% ethanol and 125 µl of 0.02% DPPH (in 99.5% ethanol). Then, the mixtures were
237 incubated in the dark for 24 h at 25 °C. The control was conducted in the same manner, expect
238 that distilled water was used instead of film sample. Finally, the absorbance of the solutions
239 was measured at 517 nm, using a UV-visible spectrophotometer. In fact, in its radical form,
240 DPPH has an absorption band at 517 nm which disappears upon reduction by antiradical
241 compounds. DPPH radical-scavenging activity was calculated as follows:

$$242 \quad \text{DPPH radical scavenging activity (\%)} = \frac{A_C + A_B - A_R}{A_C} \times 100 \quad \text{Eq (6)}$$

243 where A_C is the absorbance of the control reaction, A_R and A_B are the absorbance of film sample
244 in the reaction mixture and without addition of DPPH solution, respectively. The assay was
245 carried out in triplicate.

246 **2.4.3. Reducing power assay**

247 The capacity of the different films to reduce iron (III) was performed according to the
248 method described by Yildirim, Mavi, & Kara (2001). 500 μ l of distilled water containing 10
249 mg of each film were added to 1.25 ml of 0.2 M phosphate buffer (pH 6.6) and 1.25 ml of 1%
250 (w/v) potassium ferricyanide. After incubation at 50 °C for 3 h, 1.25 ml of 10% (w/v)
251 trichloroacetic acid were added to the mixture which was then centrifuged. 1.25 ml of the
252 supernatant of each sample were mixed with 1.25 ml of distilled water and 0.25 ml of 0.1%
253 (w/v) ferric chloride. After incubation at room temperature for 10 min, the absorbance of the
254 final solutions was measured at 700 nm. Higher absorbance of the reaction mixture showed
255 higher reducing power. The experiments were carried out in triplicate.

256 **2.4.4. Total antioxidant activity**

257 This test is based on the reduction of Mo (VI) to Mo (V) by the sample and the subsequent
258 formation of a green phosphate/Mo (V) complex at acidic pH (Prieto, Pineda, & Aguilar, 1999).
259 100 μ l of distilled water containing 10 mg of film sample were homogenized with 1 ml of
260 reagent solution (0.6 M sulphuric acid, 28 mM sodium phosphate and 4 mM ammonium
261 molybdate) and incubated at 90 °C for 90 min. The absorbance was measured at 695 nm against
262 a control solution, containing 100 μ l distilled water instead of sample. The total antioxidant
263 activity was expressed as α -tocopherol equivalents using the following equation:

$$264 \quad A = 0.011 \times C + 0.0049; R^2 = 0.987 \quad \text{Eq (7)}$$

265 where A is the absorbance at 695 nm and C is the concentration expressed as α -tocopherol
266 equivalents (μ mol/ml).

267 2.5. Statistical analysis

268 Experiments were carried out in triplicate, except films water contact angle, tickness and
269 mechanical properties analyses, which were repeated six times, and average values with
270 standard deviation errors are reported. Statistical analyses were performed with SPSS software
271 package ver. 17.0 professional edition (SPSS, Inc., Chicago, IL, USA) using ANOVA analysis
272 and differences were considered significant at p value < 0.05 .

273 3. Results and discussion

274 3.1. Polymer characterization and films preparation

275 The physicochemical characterization of chitosan (Ch) and its high molecular weight
276 (Mw) depolymerization products (CDP) C1 and C24 was carried out. The average Mw, the
277 intrinsic viscosity and the crystallinity index were lower in the CDP as compared to the native
278 chitosan Ch. However, all of them exhibited the same acetylation degree ($p > 0.05$) (**Table 1**).

279 Then, to evaluate the influence of chitosan and its derivatives (Ch, C1 and C24), as amino
280 ($-NH_2$) group donor on the physical, structural and antioxidant properties of CDP-based films,
281 glucose as carbonyl ($-C=O$) group donor was added to promote Maillard reaction (MR).

282 **Table 1:** Physicochemical characterization of chitosan and its derivatives obtained by
283 enzymatic hydrolysis of chitosan using the bacterial crude chitosanase from *B. licheniformis*
284 strain.

Polymer	Molecular weight (kDa)	Intrinsic viscosity (dl/g)	Acetylation degree (%)	Crystallinity index (%)
Ch	1244.70	7.8 ± 0.21^A	7.60 ± 0.54^A	74.40
C1	482.03	1.81 ± 0.02^B	8.12 ± 0.03^A	61.89
C24	163.56	1.25 ± 0.02^C	8.83 ± 0.33^A	51.30

285 Means with different letters (A-C) and within a column indicate significant difference ($p <$
286 0.05).

287 **3.2. Effect of MR on Films color and light barrier properties**

288 Among the basic properties of a film to be applied in the food packaging areas, optical
289 features, including color, are considered a key factor affecting the appearance of coated
290 products as well as the consumer's acceptability.

291 **3.2.1. Films color parameters**

292 The change in film's color is considered an important indicator of the occurrence and
293 extent of MR (Kchaou et al., 2019). As shown by visual observation, the unheated films,
294 supplemented or not with glucose, were colorless, transparent and homogenous, whereas, a
295 narrow change to yellow was noted regarding the color of the heated glucose-free films (**Fig.**
296 **S1**). However, the color of the MR crosslinked films changed visually turning toward dark
297 yellow. This variation was more pronounced in the film F3-Glu-90 followed by F2-Glu-90 and
298 F1-Glu-90, implying that the generation of MRP was more induced for these systems probably
299 since there was less stearic hindrance when lower Mw chitosan depolymerization products
300 (CDP) were used (Leceta et al., 2013b).

301 The final stage of MR was further evaluated by color measurement using CIELab scale
302 and L* (whiteness/darkness), a* (greenness/redness) and b* (blueness/yellowness) values
303 parameters were used to calculate total color change (ΔE^*) and browning index (BI) values.
304 Results are given in **Table 2**. Interestingly, L* values decreased significantly in the heated films
305 containing glucose, indicating that these films turn darker. Further, this decrease was more
306 noticeable in the films containing the lowest Mw-CDP (F3-Glu-90 and F2-Glu-90) as compared
307 to F1-Glu-90. However, negligible change of color has been observed for free-glucose heated
308 films, showing that the thermal treatment was not the main factor affecting the films color.
309 Darker films with lowering lightness (L*) are advantageous to prevent oxidative deterioration
310 by coating sensitive to light foods (Yang et al., 2015). The development of the dark yellowish
311 color is related to the production of dark products after 24 h of heating at 90 °C due to the

312 interactions between chitosan/CDP and glucose through MR. Indeed, conversely to a^* values
313 variations, b^* values increased significantly in the heated films as compared to the non-heated
314 ones toward the green and yellow regions, respectively, for a^* and b^* coordinates and the most
315 significant effect was obtained with the glucose-containing heated films, especially F3-Glu-90
316 ($a^* = -1.50 \pm 0.03$, $b^* = 9.15 \pm 0.27$). Such increase in b^* values was related to the higher
317 reducing end content of low Mw-CDP. Results are in accordance with those of Leceta,
318 Guerrero, & de la Caba (2013a).

319 To better understand the above-mentioned differences between blank and MR-treated
320 films, ΔE^* was determined. ΔE_1^* values, obtained by comparing the control films with the film
321 F1, showed a weak increase to slightly yellowish color for the films F2 and F3 due to the use
322 of low Mw-CDP. Further, the addition of glucose slightly increased the total color change in
323 all the control films. Furthermore, ΔE_2^* values were measured, taking the control films (F1, F2
324 and F3) as a point of reference for each Mw-chitosan-based film, in order to assess the observed
325 differences between heated films and the non-heated ones. Results showed that ΔE_2^* increased
326 slightly in the free-glucose heated films, but increased significantly in the heated glucose
327 containing films to 9.75, 13.54 and 14.31 for F1-Glu-90, F2-Glu-90 and F3-Glu-90,
328 respectively. This variation pointed that color change was inversely proportional to the Mw of
329 used CDP, generating more colored films when lowest Mw-CDP were used. Similar behavior
330 of higher color change for heated lower Mw-chitosan-based films as compared to unheated ones
331 and to heated higher Mw-chitosan-based films, was reported by Leceta et al. (2013a). Such
332 results of ΔE_1^* and ΔE_2^* values indicated that MR resulted films are dark-colored and have
333 stronger barrier ability in the visible region than that of non-heated films. This color change of
334 the films conjugated with glucose could imply that the film structure also changed as a result
335 of thermal treatment during 24 h at 90 °C.

336 Additionally, the BI is a good indicator of the changes in color due to the MRP
 337 (Matiacevich & Pilar Buera, 2006). As shown in **Table 2**, low BI values were obtained in the
 338 free-glucose treated films. However, similarly to the trend of ΔE^* , the BI of heated films
 339 conjugated with glucose increased significantly and proportionally to the decrease of the Mw
 340 of CDP and reached 12.49 ± 0.12 , 50.13 ± 0.18 and 71.33 ± 3.05 for the films F1-Glu-90, F2-
 341 Glu-90 and F3-Glu-90, respectively.

342 **Table 2:** Color parameters (L^* , a^* and b^*), total color change (ΔE_1^* and ΔE_2^*) and browning
 343 index (BI) of the different Mw-chitosan based films with and without glucose and thermal
 344 treatment.

Films	L^*	a^*	b^*	ΔE_1^*	ΔE_2^*	BI
F1	28.36 ± 1.09^A	-0.45 ± 0.05^A	-0.46 ± 0.07^I	-	-	-
F1-90	27.30 ± 0.85^{AB}	-0.60 ± 0.03^B	0.64 ± 0.04^G		1.68 ± 0.36^B	0.70 ± 0.11^E
F1-Glu	27.95 ± 0.19^{AB}	-0.60 ± 0.01^B	-0.35 ± 0.09^I	0.47 ± 0.15^D	0.47 ± 0.15^B	-
F1-Glu-90	19.18 ± 0.90^C	-0.67 ± 0.04^{BC}	2.78 ± 0.06^C		9.75 ± 0.82^A	12.49 ± 0.12^C
F2	28.29 ± 0.05^A	-0.74 ± 0.03^{CD}	0.18 ± 0.05^H	0.71 ± 0.02^D	-	-
F2-90	27.90 ± 0.50^{AB}	-0.87 ± 0.03^E	1.75 ± 0.14^D		1.70 ± 0.01^B	3.98 ± 0.50^{DE}
F2-Glu	27.92 ± 0.05^{AB}	-0.80 ± 0.03^{DE}	0.84 ± 0.04^{FG}	1.41 ± 0.01^C	0.76 ± 0.01^C	-
F2-Glu-90	16.89 ± 0.10^D	-1.17 ± 0.01^G	7.48 ± 0.02^B		13.54 ± 0.07^A	50.13 ± 0.18^B
F3	27.87 ± 0.18^{AB}	-1.01 ± 0.03^F	1.20 ± 0.16^{EF}	1.83 ± 0.09^B	-	-
F3-90	26.48 ± 0.08^B	-1.19 ± 0.03^G	2.39 ± 0.02^C		1.84 ± 0.05^B	5.82 ± 0.13^D
F3-Glu	26.89 ± 0.08^{AB}	-1.21 ± 0.01^G	1.29 ± 0.27^E	2.36 ± 0.15^A	0.95 ± 0.04^C	-
F3-Glu-90	15.99 ± 0.05^D	-1.50 ± 0.03^H	9.15 ± 0.27^A		14.31 ± 0.1^A	71.33 ± 3.05^A

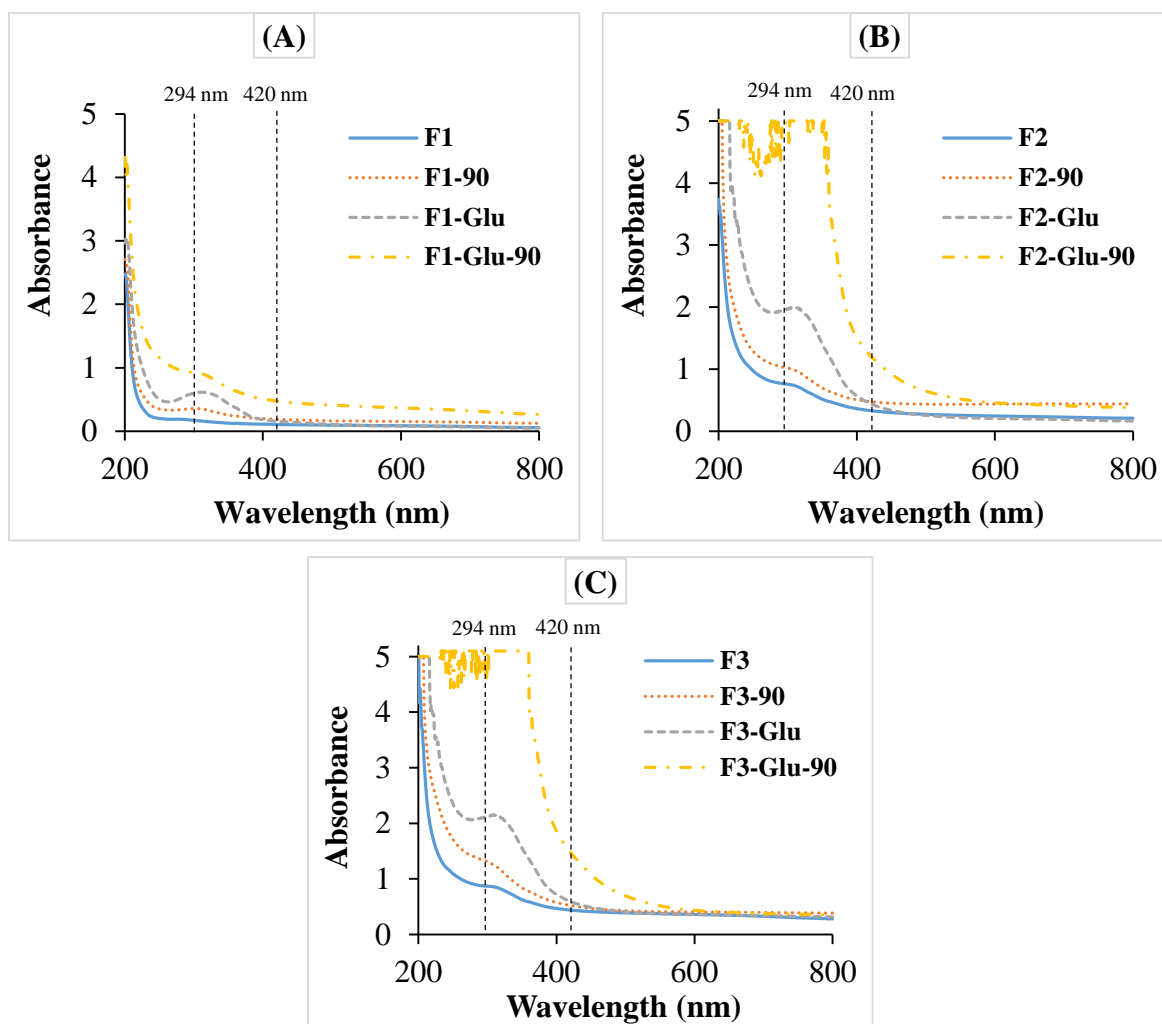
345 Values are means \pm standard deviation ($n = 3$). Means with different letters (A-J) and within a
 346 column indicate significant difference ($p < 0.05$). ΔE_1^* was calculated regarding to F1 and ΔE_2^*
 347 was the change of color measured as compared to each control film (F1, F2 and F3).

348 3.2.2. Ultraviolet-visible light spectroscopy

349 An effective packaging intended to food applications should demonstrate light barrier
350 behavior to protect the packaged food from the degradative effects of light, particularly UV-
351 light, which generates chemical reactions catalyzation, accelerating the deterioration of food
352 and thus affecting ultimately the food quality as well as the consumer acceptance. Therefore,
353 the UV-visible spectroscopy was investigated in the range of 200-800 nm in order to study the
354 effect of chitosan/CDP supplementation in the extent of MR in film matrix, by analyzing their
355 light barrier properties, and to correlate color changes with the formation of MRP at different
356 stages. As it can be seen in **Fig. 1**, the spectra of the different Mw chitosan-based films showed
357 good barrier properties to light in the UV region, with a slightly better effect in the film F3,
358 containing the lower Mw-CDP, followed by F2 as compared to F1. Further, a slight increase of
359 the UV absorption of the heated glucose-free films (F1-90, F2-90 and F3-90) was detected, as
360 compared to the control unheated ones (F1, F2 and F3). This slight modification is probably
361 due to the caramelization reaction caused by direct heating of carbohydrates (Li et al., 2014)
362 and it was more pronounced in the film F3-90, followed by F2-90, as compared to F1-90. Such
363 results were similar to those reported by Leceta et al. (2013b) who reported the same trend of
364 better barrier properties in low Mw chitosan-based films before and after treatment at 105 °C,
365 as compared to higher Mw chitosan films.

366 In contrast, after glucose addition, a significant change of absorbance was observed when
367 the films were heated, as compared to the unheated ones, especially when lower Mw-CDP were
368 used. Whereas, the absorbance (A) increases noticeably, in the range of 250-450 nm, in the
369 films F3-Glu-90 followed by F2-Glu-90 and F1-Glu-90. This obvious modification is a result
370 of MR which is a condensation reaction between nitrogen-containing compounds of chitosan
371 and its derivatives and the carbonyl group of reducing sugars (glucose) (Li et al., 2014). Such
372 reaction is a cross-linking process which follows a complex mechanism with three major stages.
373 In the initial stage, the sugar-amine conjugation allowed to the development of Amadori

374 colorless products via rearrangement. The reaction became yellow with high UV-absorbance at
375 the intermediate stage. Whereas, brown compounds are formed in the final stage from aldol
376 condensation and aldehyde amide polymerization along with the formation of heterocyclic
377 nitrogen compounds (Gullón et al., 2016). Consequently, the color of conjugated products may
378 be a direct and easy indication of MR progress. UV-absorbance ($A_{294\text{ nm}}$) and brown color (A_{420}
379 nm) are typical indicators of colorless intermediate compounds and final browning compounds,
380 respectively. The changes of $A_{294\text{ nm}}$ and $A_{420\text{ nm}}$ of MR-crosslinked CDP-based films were
381 shown in **Fig. 1**. It could be found that, in all cases, the values of $A_{294\text{ nm}}$ were higher than those
382 obtained at 420 nm, which is characteristic index of the formation of intermediate compounds
383 of the MR. Similarly, Kosaraju et al. (2010) stated that the thermal treatment of glucose-added
384 chitosan (Mw of 810 kDa) resulted in higher rates of intermediate browning products than final
385 browning products. Moreover, the $A_{280\text{ nm}}$ and $A_{420\text{ nm}}$ of the film F3-Glu-90 were higher than
386 those of the film F2-Glu-90 and especially F1-Glu-90, suggesting that MR rate was influenced
387 by the Mw of CDP-based film. This difference to induce MR regarding the Mw of
388 chitosan/CDP is due to the fact that high Mw-chitosan chains are more static, owing to its higher
389 length and compact structure, which prevent the proximity between amino and carbonyl groups
390 to react through MR (Leceta et al., 2013b). Therefore, MRP-containing films, especially F3-
391 Glu-90 followed by F2-Glu-90, have excellent light barrier properties, suggesting their potential
392 effect on the retardation of product oxidation induced by UV-light. These findings agreed with
393 color measurement which indicates that color change was more pronounced for lower Mw
394 CDP-based films.



395

396

397 **Figure 1:** UV-vis spectra of chitosan (A), CDP-C1 (B) or CDP-C24 (C) based-films, with and
 398 without glucose and before and after thermal treatment through MR at 90 °C during 24 h.

399 3.3. Effect of MR on films functional properties

400 The functional properties of CDP-based films as influenced by MR, including water
 401 content (WC), water solubility (WS) and water contact angle (WCA) were evaluated and results
 402 are illustrated in **Table 3** and **Fig. S2**.

403 **Table 3:** Water content (WC), water solubility (WS), water contact angle (WCA at t = 10 and
 404 20 s), thickness and mechanical properties (TS and EAB) of chitosan or CDP based films
 405 containing or not glucose before and after thermal treatment.

Water resistance properties

Mechanical properties

Films	WC (%)	WS (%)	WCA (°)		Thickness (µm)	EAB (%)	TS (MPa)
			T _{10 s}	T _{20 s}			
F1	12.28 ± 0.16 ^{BCD}	12.12 ± 1.01 ^E	108.60 ± 2.24 ^A	106.93 ± 2.26 ^A	0.027 ± 0.002 ^A	15.26 ± 0.74 ^{AB}	17.99 ± 0.25 ^A
F1-90	10.33 ± 0.33 ^E	9.33 ± 0.50 ^F	95.70 ± 0.62 ^B	95.10 ± 0.94 ^B	0.028 ± 0.004 ^A	15.50 ± 0.85 ^A	18.44 ± 0.73 ^A
F1-Glu	13.20 ± 0.18 ^{ABC}	14.48 ± 0.30 ^D	95.91 ± 1.71 ^B	94.14 ± 1.49 ^B	0.026 ± 0.003 ^A	13.91 ± 0.01 ^{BC}	17.57 ± 1.22 ^{AB}
F1-Glu-90	10.91 ± 0.21 ^{CDE}	9.54 ± 0.71 ^F	87.16 ± 2.35 ^C	84.26 ± 2.74 ^C	0.027 ± 0.007 ^A	15.52 ± 0.85 ^A	18.56 ± 0.59 ^A
F2	12.41 ± 0.37 ^{BCD}	17.93 ± 0.85 ^C	65.66 ± 3.37 ^D	61.39 ± 2.35 ^D	0.025 ± 0.002 ^A	12.23 ± 0.52 ^{DE}	16.72 ± 0.46 ^{ABC}
F2-90	11.08 ± 0.58 ^{DE}	11.26 ± 0.64 ^{EF}	61.86 ± 1.84 ^{DE}	58.99 ± 1.78 ^{DE}	0.026 ± 0.001 ^A	13.31 ± 0.27 ^{CD}	17.65 ± 0.39 ^{AB}
F2-Glu	13.85 ± 0.35 ^{AB}	20.93 ± 0.80 ^B	62.45 ± 2.50 ^{DE}	59.54 ± 2.56 ^{DE}	0.027 ± 0.008 ^A	11.47 ± 0.01 ^E	14.80 ± 0.01 ^{CD}
F2-Glu-90	11.12 ± 0.38 ^{DE}	10.12 ± 0.88 ^{EF}	56.60 ± 2.86 ^{EF}	53.46 ± 3.43 ^{EF}	0.027 ± 0.003 ^A	13.88 ± 0.4 ^{BC}	15.57 ± 0.75 ^{BCD}
F3	13.16 ± 0.09 ^{CDE}	20.26 ± 1.03 ^B	59.83 ± 3.17 ^{DE}	57.62 ± 4.01 ^{DE}	0.021 ± 0.003 ^A	8.39 ± 0.19 ^G	15.06 ± 0.85 ^{CD}
F3-90	11.12 ± 0.32 ^{DE}	15.98 ± 0.70 ^{CD}	57.07 ± 1.92 ^{EF}	53.43 ± 1.74 ^{EF}	0.023 ± 0.005 ^A	9.88 ± 0.17 ^{FG}	16.43 ± 0.45 ^{ABCD}
F3-Glu	14.28 ± 0.58 ^A	23.68 ± 0.30 ^A	50.24 ± 1.16 ^{FG}	47.76 ± 1.19 ^{FG}	0.027 ± 0.009 ^A	8.35 ± 0.13 ^G	14.36 ± 0.65 ^D
F3-Glu-90	11.29 ± 0.46 ^{DE}	11.39 ± 0.51 ^{EF}	45.26 ± 1.02 ^G	41.50 ± 1.18 ^G	0.027 ± 0.002 ^A	10.71 ± 0.42 ^{EF}	14.90 ± 0.17 ^{CD}

406 Values are means ± standard deviation (n = 3). Means with different letters (A-G) and within a
407 column indicate significant difference ($p < 0.05$).

408 3.3.1. Water content measurement

409 WC of the films as packaging material, which correspond to the total void volume
410 occupied by water molecules, is an important factor affecting the shelf life of packaged food
411 (Hazaveh, Mohammadi Nafchi, & Abbaspour, 2015). As shown in **Table 3**, the WC of all
412 unheated films increased when glucose was added, as compared to free-glucose-based films.
413 Similarly, Kchaou et al. (2018) reported an increase of WC in the non-heated gelatin films as a
414 result of glucose addition. Further, the WC of the films containing the lowest Mw-CDP (C24)
415 was slightly higher than those of the films containing the high Mw-CDP (C1) and the native
416 chitosan. Such increase in WC could be explained by the well-known hygroscopicity of
417 saccharides. After induction of the MR (heat treatment at 90 °C), the WC of all films decreased
418 significantly as compared to the unheated ones. The decrease of WC of the films F1-Glu-90,
419 F2-Glu-90 and F3-Glu-90, as compared to the glucose-based films may be explained by the
420 interaction between the amino group of chitosan, C1 and C24, respectively, and the carbonyl
421 group of glucose through MR.

422 3.3.2. Study of water solubility

423 WS, which provides insight into the behavior of the film in an aqueous environment, is
424 considered a crucial feature in defining the applications of biopolymeric films. **Table 3** shows
425 the WS values of prepared films. Control CDP-based films (F2 and F3) showed significant
426 higher WS values, as compared to the chitosan-based film (F1). Such difference may be
427 attributed to the Mw variation among chitosan and CDP samples which thereby affects their
428 WS, being 15.09, 30.3 and 34.79 % for chitosan, C1 and C24, respectively (Affes et al., 2020b).
429 Further, glucose addition in the control films increased significantly the WS, as compared to
430 free-glucose films. This result was in agreement with Kchaou et al. (2018) who reported that
431 glucose addition increased the WS of control fish gelatin films. However, when films were
432 heat-treated at 90 °C, WS values decreased significantly ($p < 0.05$), indicating a change in their
433 chemical structure. This decrease was more pronounced in the films containing glucose and
434 especially in the lower Mw CDP-based films. Therefore, the cross-linking induced by heating
435 and glucose addition through MR could be an effective method to control the WS of
436 chitosan/CDP-based films, providing an important functional property of those films, as it was
437 reported by other authors (Leceta et al., 2013b). Similarly, Fernández-de Castro et al. (2016)
438 demonstrated that chitosan-oligosaccharides films showed higher WS values than chitosan
439 films, when treated at 105 °C. In the same context, they stated that the decrease of soluble
440 matter in thermally-treated films was related to the decrease of free amino groups, as compared
441 to unheated films. In this context, Etxabide, Urdanpilleta, Guerrero, & de la Caba (2015)
442 reported that lactose addition reduced significantly the solubility of fish gelatin film after
443 heating at 105 °C.

444 3.3.3. Water contact angle assessment

445 The surface resistance of a film to water wetting and adhesion is an important property
446 which is affected by its chemical composition and surface morphology (Bharathidasan,

447 Narayanan, Sathyanaryanan, & Sreejakumari, 2015). This property was studied by water
448 contact angle (WCA) measurement which is an indicator of the degree of
449 hydrophilicity/hydrophobicity of the film surface. The final state of a water drop informs about
450 the surface wettability.

451 Results illustrated in **Fig. S2** and **Table 3** show the variation of WCA as a function of
452 chitosan or CDP-Mw, glucose addition and thermal treatment for the different films. Firstly, in
453 all films, as compared to $T_{10\text{ s}}$, a slight decrease of WCA was obtained at $T_{20\text{ s}}$ due to the
454 evaporation of the water drop. Further, chitosan-based film (F1) showed the highest WCA
455 values above 108.60 and 106.93 ° at $T_{10\text{ s}}$ and $T_{20\text{ s}}$, respectively. These values agree with the
456 results obtained by Leceta et al. (2013b) and de Britto & Assis (2007) for chitosan-based films
457 (around 105 and 100 °, respectively). Except F1-Glu-90, Chitosan-based films were considered
458 as hydrophobic as they exhibit WCA values higher than 90 °. However, there is a significant
459 decrease in WCA values in the films F2 and F3 containing lower Mw-CDP, as compared to F1,
460 probably related to the higher moisture contents of these films, thus indicating more ability to
461 absorb water and allowing to higher hydrophilicity. This result was in contradiction with that
462 of Leceta et al. (2013a) who stated that the Mw of chitosan did not affect significantly WCA
463 values. Furthermore, in all cases, WCA decreased slightly in the control films conjugated with
464 glucose. This variation is probably explained by the great affinity of free glucose, not yet
465 involved in MR, towards water. After thermal treatment, WCA tends to decrease significantly
466 for all the films as compared to the control ones, indicating thereby that heating leads to an
467 increase of chitosan or CDP films hydrophilicity. Similarly, Leceta et al. (2013b) and Kchaou
468 et al. (2019) reported that the heat-treatment of chitosan and gelatin films, respectively, caused
469 a slight decrease in WCA values, due to changes in the conformation of molecules and to the
470 exposure of the hydrophilic groups toward the surface.

471 **3.4. Films thickness and mechanical properties of CDP-based MR-treated films**

472 Maintainig their integrity is very important for coating applied for food packaging, to
473 endure the distribution, treatment and storage occuring stress. In order to have information
474 about flexibilty and stretchability of the different films, their mechanical properties, regarding
475 tensile strenght (TS) and elongation at break (EAB), were evaluated. Firstly, results from **Table**
476 **3** show that all films had similar thickness, around 0.026 μm ($p > 0.05$).

477 Further, as can be seen, among all film samples, the group of chitosan-based films showed
478 the highest TS and EAB ($p < 0.05$) values than CDP-based films groups, thus indicating that
479 the decrease in Mw of CDP leads to a notably decrease in films mechanical properties.
480 According to the literature, comparison of mechanical properties of chitosan-based films is
481 difficult related to the variations in Mw, acetylation degree, concentration of chitosan and
482 plasticizer, as well as film preparation and test conditions. Similarly, Leceta et al. (2013a)
483 reported that films mechanical properties were related to chitosan physicochemical
484 characteristic and contrarily to our results, they demonstrate that low Mw chitosan-based films
485 exhibited lower TS but higher EAB than higher Mw chitosan films. Furthermore, the addition
486 of glucose resulted in a decrease of both TS and EAB of the three unheated different Mw-
487 chitosan-based films. This decrease is in contradiction with results of Kchaou et al. (2018) who
488 stated that the addition of glucose in gelatin-based films did not affect the mechanical
489 parameters of unheated films. However, a significant increase of TS and EAB values was
490 observed after thermal treatment of the films F1-90, F2-90 and F3-90, as compared to the free-
491 glucose control films, and after MR in the films F1-Glu-90, F2-Glu-90 and F3-Glu-90,
492 regarding to control glucose-containing films. The best properties were observed in the film
493 F1-90, followed by F1-Glu-90 and F2-90 ($p < 0.05$). Our results disagreed with those reported
494 by of Hosseini, Razavi, & Mousavi (2009) and Affes et al. (2020a) who suggested that the
495 increase in the EAB of the films can be ascribed to the increased WC values. According to the
496 literature, the improvement of mechanical properties of heated films is highly dependent on the

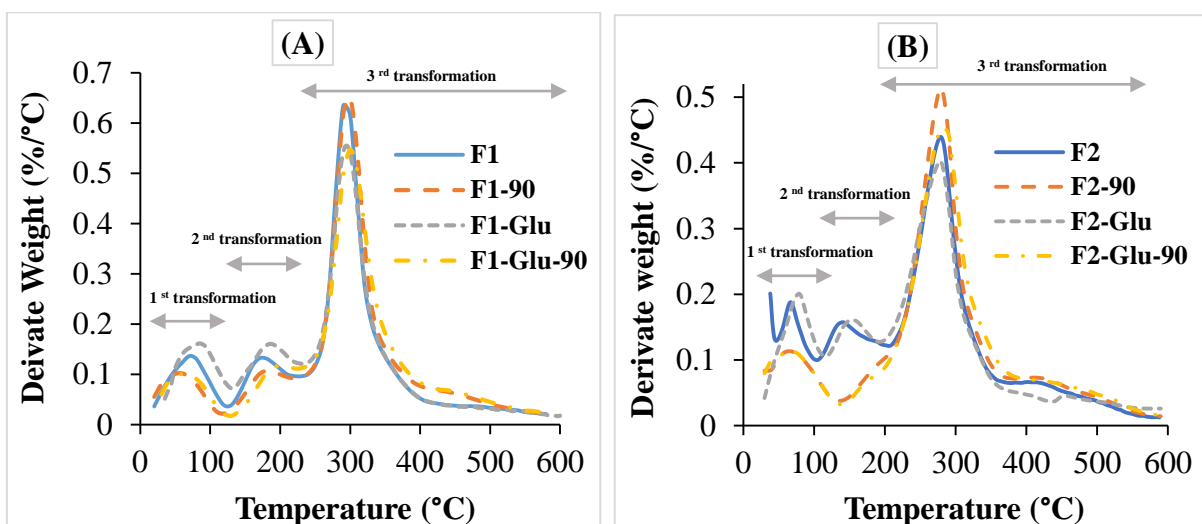
497 distribution and density of both intermolecular and intramolecular interactions in the network
498 created in chitosan films, thus leading to the formation of more compact structure induced by
499 crosslinking through MR (Park et al., 1999).

500 **3.5. Effect of MR crosslinking on the thermal behavior of CDP-based films**

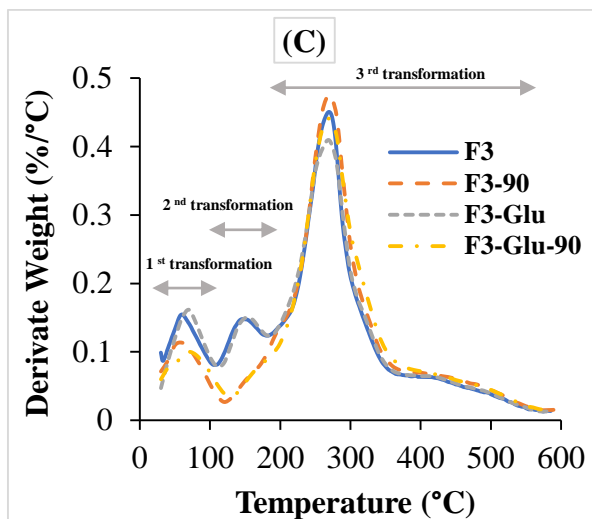
501 The thermal stability of chitosan-based films crosslinked or not with glucose was assessed
502 by TGA analysis, in a temperature range of 30-600 °C, in order to study the changes promoted
503 by the effects of thermal treatment and chitosan Mw variation on the interactions between polar
504 groups. The weight loss, temperature of maximum degradation (T_{max}) and final residual mass
505 of the films, determined from TGA thermograms (**Fig. 2**), are illustrated in **Table 4**.

506 DTGA curves of control chitosan or CDP-based films with and without glucose indicated
507 three steps of transformations corresponding to the main stages of weight loss. The first stage
508 observed from 30 to 140 °C was related to the loss of free and bound water. In this stage, the
509 weight loss ranged from 9 to 12% with a slight higher values in the films containing glucose as
510 compared to the free-glucose films. However, for the heated films, the weight loss values
511 decreased slightly after 24 h of thermal treatment at 90 °C and ranged from 6 to 9%. Such
512 variations correlate with the results of WC (**Table 2**) which indicates that glucose-containing
513 films (F1-Glu, F2-Glu and F3-Glu) possess higher WC values than the free ones and the treated
514 films present lower WC than the non-heated ones. A second small weight loss (about 10%) was
515 observed at approximately 140-240 °C. It is probably related to entrapped water through
516 hydrogen bonds and the elimination reaction of NH_3 , as mentioned by Martins, Cerqueira, &
517 Vicente (2012) or to the evaporation of glycerol, as suggested by Leceta et al. (2013b). In the
518 case of the heated films, the weight loss in this stage decreased in the chitosan-based films (F1-
519 90 and F1-Glu-90) and disappeared in the films containing low Mw-CDP (C1 and C24), thus
520 indicating a change in the structure of films after heat treatment.

521 The third stage corresponds to the degradation or the decomposition of chitosan and CDP
 522 chains (Martins et al., 2012). This transformation revealed the main stage of weight loss,
 523 between 45 and 49% for unheated films. Higher weight loss values were obtained for heated
 524 films from 51 to 57%. Regarding the T_{max} , relative values showed that the glucose incorporation
 525 does not affect the temperature of degradation of control chitosan or CDP-based films.
 526 However, thermal treatment allows to a slight increase in the T_{max} of the films with and without
 527 glucose. The better thermal resistance in treated free-glucose films could be due to the
 528 generation of new interactions between chitosan chains. Whereas, the development of MRP in
 529 heated chitosan-glucose-based films may explain the increase of their thermal stability. Further,
 530 chitosan-based films revealed higher T_{max} values, about 300 °C, as compared to those
 531 containing CDP-C24 and CDP-C1, around 280 and 270 °C, respectively. The residual weight
 532 at 600 °C was higher when low Mw-CDP were used and for the heated films regarding the
 533 unheated ones. These results confirm that thermal treatment and MR modified the structure of
 534 the films leading to a more thermally stable matrix which enhance the films functional
 535 properties (Leceta et al., 2013b), as shown by the decrease of WS values.



536



537

538 **Figure 2:** DTGA thermograms of chitosan (A) and chitosan derivatives, CDP-C1 (B) and CDP-
 539 C24 (C), based films with and without glucose before and after thermal treatment at 90 °C.

540 **Table 4:** Weight loss, maximal degradation temperature (T_{max}) and residue as function of
 541 degradation temperatures, based on the TGA thermograms of chitosan or CDP based films
 542 conjugated or not with glucose through Maillard reaction (MR) at 90 °C as function of time (0
 543 and 24 h).

Films	Temperature range for weight loss at different stages (°C)	Weight loss (%)		Residual weight (%) at 600 °C	T_{max} (°C)
		Partial	Total		
F1	30.0 - 135.1	9.67	68.57	31.43	297.00
	135.1 - 241.6	10.6			
	241.6 - 600.0	48.3			
F1-90	30.0 - 131.4	7.2	67.80	32.20	298.15
	131.4 - 240	8.8			
	240 - 600.0	51.8			
F1-Glu	30.0 - 127.31	11.71	69.63	30.37	298.10
	127.31 - 228.59	12.72			
	231.3 - 600.0	45.2			
F1-Glu-90	30.0 - 128.4	6.95	66.90	33.10	299.70
	128.4 - 231.3	8.5			
	231.0 - 600.0	51.45			
F2	30 - 106.0	10.5	68.37	31.63	279.12
	106.0 - 208.3	13.7			
	208.3 - 600.0	44.17			
F2-90	30.0 - 139.3	9.2	63.92	36.08	280.93

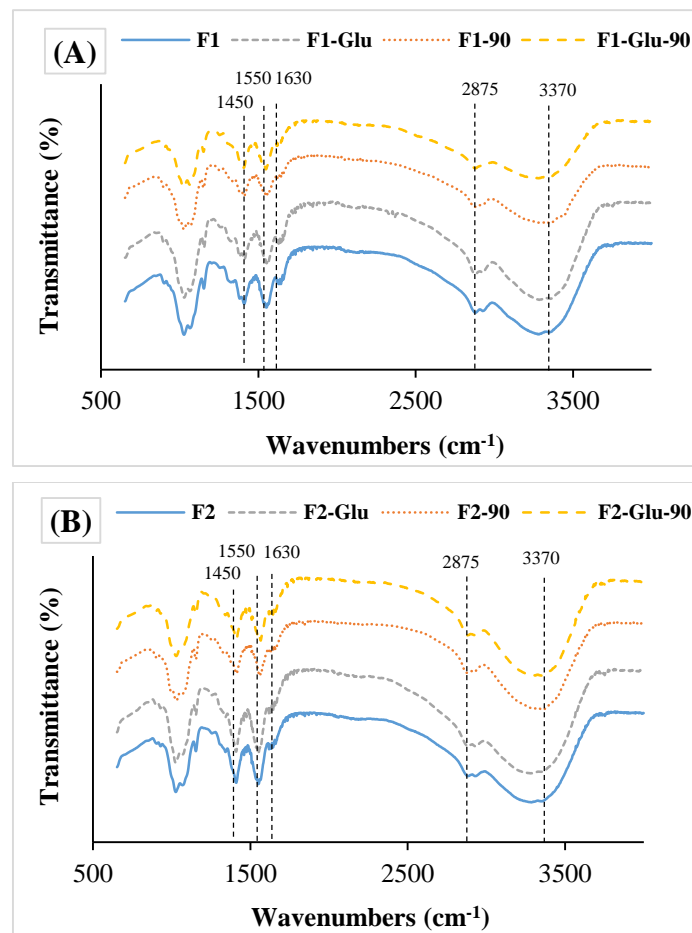
	139.3 – 600.0	54.72			
F2-Glu	30.0 – 115.7	12.04	67.29	32.71	278.10
	115.7 – 193.8	10.88			
	193.8 – 600.0	44.37			
F2-Glu-90	30.0 – 128.4	8.6	64.04	35.96	279.12
	128.4 – 600.0	55.44			
F3	30.0 - 112.1	9.64	68.05	31.95	270.88
	112.1 - 186.5	9.3			
	186.5 – 600.0	49.11			
F3-90	30 - 119.3	7.3	64.40	35.60	271.25
	119.3 - 600.0	57.1			
F3-Glu	30 - 113.3	9.78	64.87	32.13	270.64
	113.3 - 187.7	9.41			
	187.7 - 600.0	48.68			
F3-Glu-90	30 – 130.2	7.03	63.50	36.50	271.64
	130.2 – 600.0	56.47			

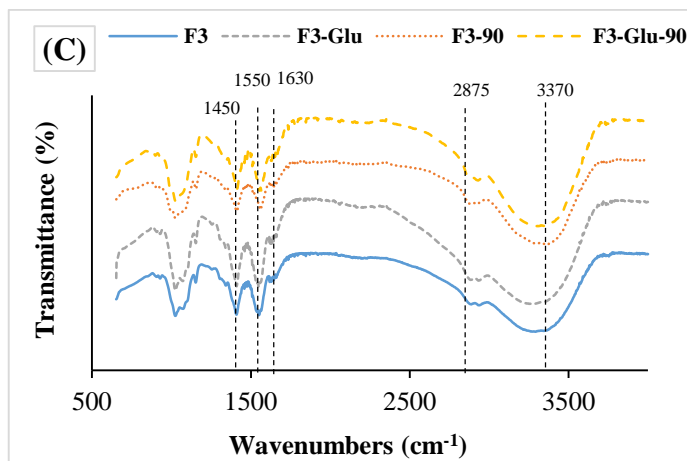
544

545 3.6. Infrared spectroscopic analysis

546 Chemical bond modifications, following the establishment of interactions between
547 functional groups in chitosan or CDP-based films due to glucose addition and MR induction,
548 were studied using ATR–FTIR spectroscopy. FTIR spectra of the films at 0 and 24 h of heating
549 at 90 °C are given in **Fig. 3**. As it can be seen, all spectra revealed the same characteristic peaks.
550 A broad absorption peak was observed at 3370 cm⁻¹ which indicates the stretching vibration of
551 the hydroxyl groups (O–H) and the intramolecular hydrogen bonding of chitosan molecules.
552 The characteristic signals of the CH stretching were detected at around 2875 cm⁻¹. The peaks
553 at around 1630, 1550, and 1450 cm⁻¹ were attributed to C=O stretching (amide I), N–H bending
554 (amide II) and C–CH₃ distorting vibration, respectively. Further, glucose addition to the varying
555 Mw-chitosan/CDP-based films did not cause significant difference in the spectra in terms of
556 the location of the bands. Moreover, in the spectra of the control unheated films, the intensity
557 of the band of amide I at 1630 cm⁻¹ was always lower than that of the band of the amide II at
558 1550 cm⁻¹, regardless of the Mw of chitosan/CDP, as a consequence of the presence of available

559 protonated amine groups ($-\text{NH}_3^+$) produced in the evaporation of solvent to form the films
560 (Fernández-de Castro et al., 2016). However, thermal treatment of the films at 90 °C reduced
561 the difference in the intensity of these two bands and the intensity of the band at 1550 cm^{-1}
562 become smaller, indicating the successful interaction, promoted by temperature, between
563 carbonyl and amine groups in the same chitosan chain, as well as between the carbonyl group
564 of glucose and amine group of chitosan for the films containing glucose, through crosslinking
565 and MR. This is in agreement with the decrease of WS observed for heat-treated films. Results
566 were consistent with those of Fernández-de Castro et al. (2016) and Gullón et al. (2016) in
567 which the same behavior was observed when chitosan films and chitosan polymer sample,
568 respectively, were thermally treated.





571
 572 **Figure 3:** FTIR spectra of chitosan (A), CDP-C1 (B) and CDP-C24 (C) films containing or not
 573 glucose, before and after heating at 90 °C during 24 h.

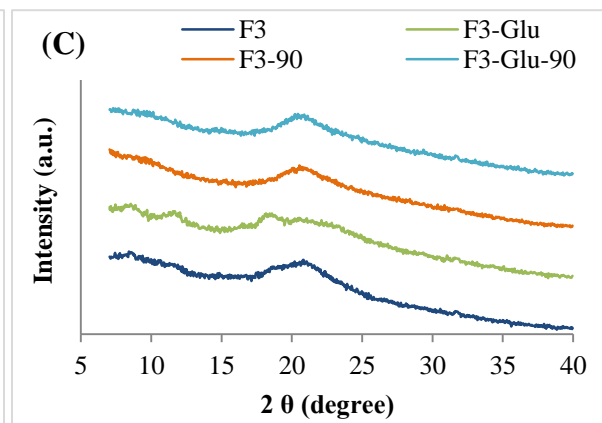
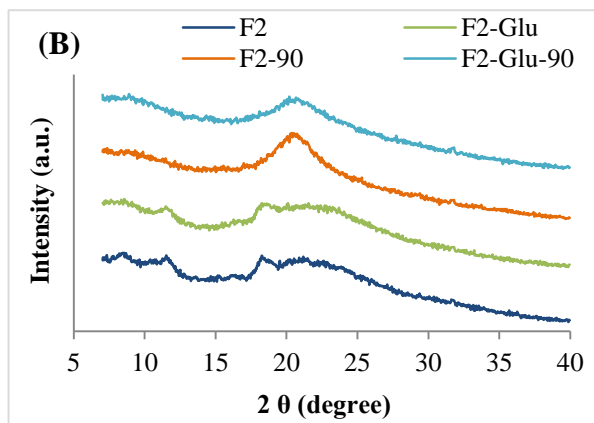
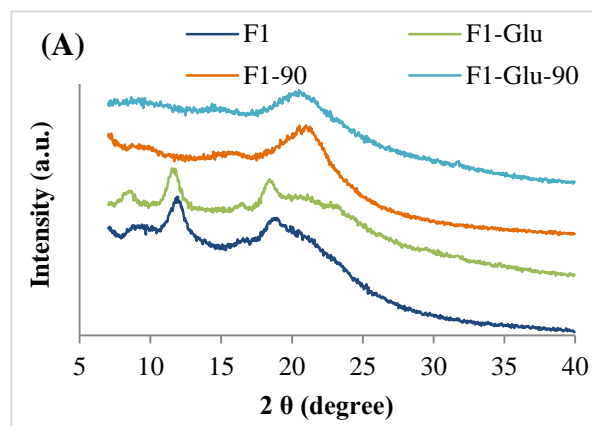
574 3.7. Structural properties of MR crosslinked CDP-based films

575 3.7.1. X-ray diffraction analysis

576 The X-ray diffraction (XRD) analysis was assessed in order to study the crystal lattice
 577 arrangements, the structural modifications and the molecular conformation changes of the
 578 prepared films caused by thermal treatment and MR. The X-ray diffractograms of chitosan and
 579 CDP-based films are shown in **Fig. 4**. Chitosan-based film (F1) exhibited a semi-crystalline
 580 structure with two main diffraction peaks at 2θ around 12 and 20 °. These characteristics peaks
 581 correspond to those of chitosan sample ($2\theta = 10$ and 20 °) (Affes et al., 2020b), with a slight
 582 shift of the first peak position from $2\theta = 10$ to 12 °, corresponding to the hydrated polymorph
 583 structure of chitosan. Similar chitosan-based films pattern was obtained by Rivero et al. (2012).

584 The crystallinity of the CDP-based films F2 and F3 decreased, as compared to the film
 585 F1, showing a less intense peak at $2\theta = 20$ °, whereas, the peak at 12 ° highly decreased in the
 586 film F2 and disappeared in the film F3. The low crystallinity of these films containing low Mw-
 587 CDP was attributed to the amorphous structure (Affes et al., 2020b) and low crystallinity index
 588 values of CDP, as compared to native chitosan (**Table1**). Further, the three control unheated
 589 glucose-containing films showed the same patterns as the free-glucose films.

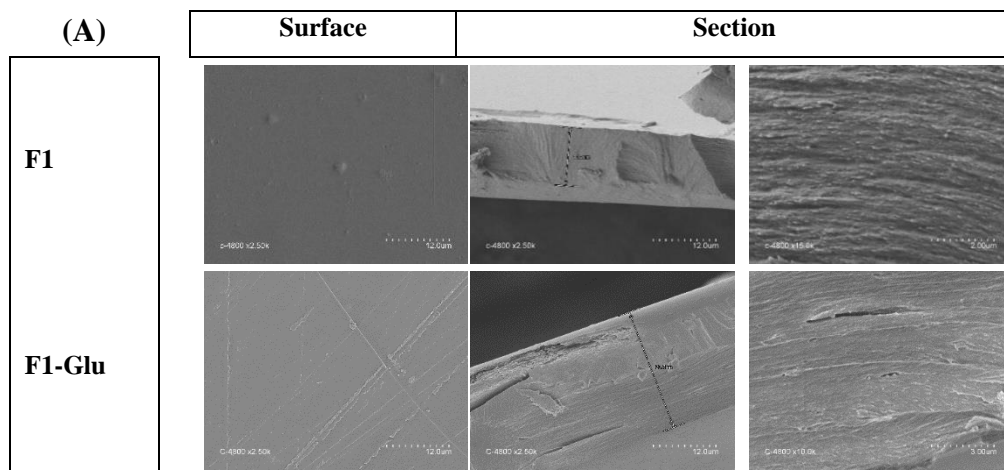
590 For heated films at 90 °C, the diffractograms showed a decrease in the intensity of the
591 peak at about 20 ° (2 θ), as compared to the control films. Moreover, the intensity of this peak
592 was lower in the heated films containing glucose regarding to free-glucose heated films, as well
593 as in the heated films containing low Mw-CDP, as compared to those containing chitosan.
594 However, the small peak at around 12 ° disappeared in all the thermally-treated films. Similarly,
595 Leceta et al. (2013b) and Rivero et al. (2012) reported that the first peak of chitosan film
596 disappeared by thermal treatment. From these diffractograms, it is obvious that chitosan films
597 are more crystalline than CDP films and that heated films had lower crystallinity than non-
598 heated films. The decrease of the crystallinity by thermal treatment could be related to the
599 reduction of intermolecular interactions among chitosan chains due to the formation of cross-
600 links through MR. Similarly, Leceta et al. (2013b) observed that chitosan film structure was
601 influenced by the effect of temperature.



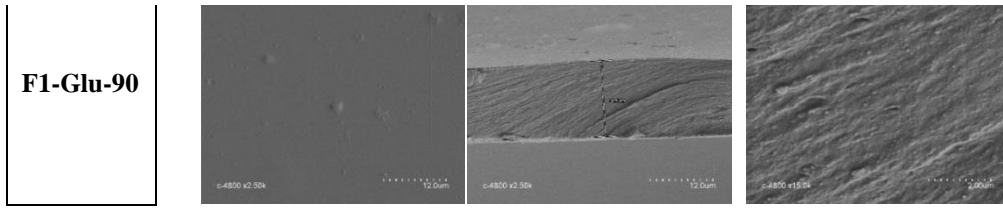
604 **Figure 4:** X-ray diffractograms of heat treated and non-treated chitosan (A) CDP-C1 (B) and
 605 CDP-C2 (C) based films with and without glucose.

606 **3.7.2. Films microstructure**

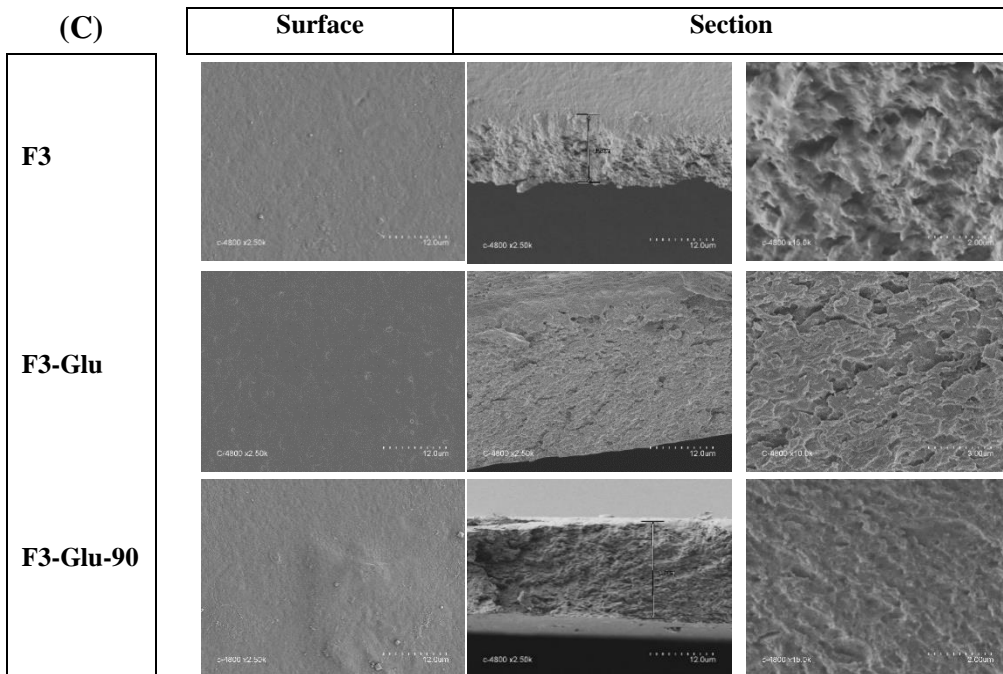
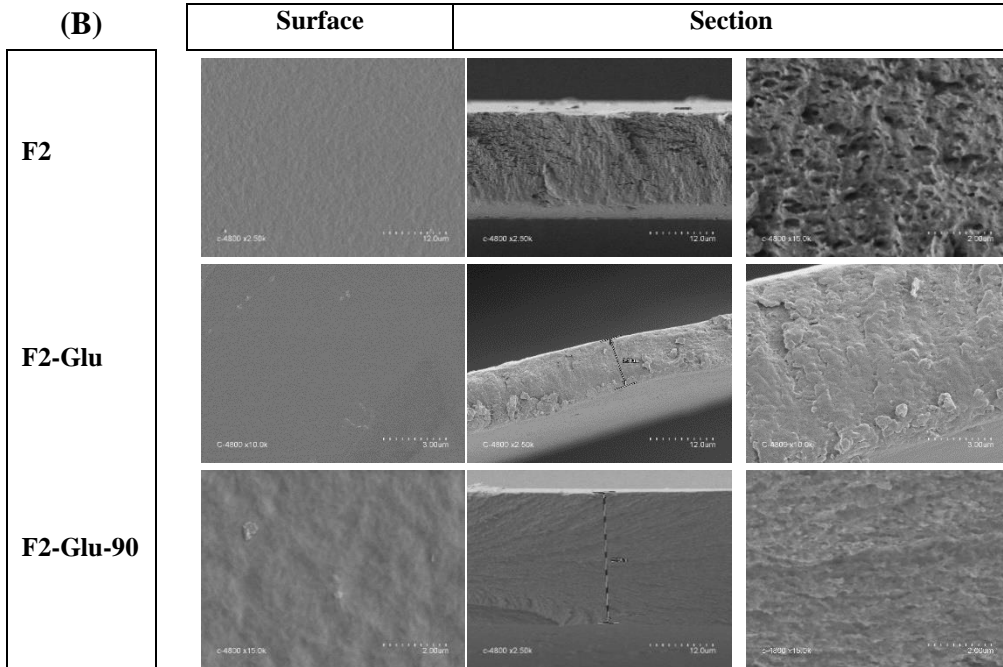
607 Surface electron microscopy (SEM) analysis was carried out in order to assess the
 608 microstructural modifications of the elaborated films, as a function of chitosan/CDP Mw,
 609 glucose addition and cross-linking reaction, allowing a better understanding of polymers film-
 610 forming behavior. SEM micrographs illustrated in **Fig. 5** showed that, in all films, the surface
 611 was flat, compact, smooth and homogenous without apparent porosity. Further, cross-sectional
 612 images of the control films with and without glucose showed a stratified structure, with an
 613 increase of the homogeneity and order of films as the Mw of chitosan-based film was higher.
 614 Similarly, Fernández-de Castro et al. (2016) reported that chitosan and chitosan-
 615 oligosaccharides-based films had homogenous microstructure with relatively roughness.
 616 However, a more compact structure was illustrated in the cross-sections of the heated films (F1-
 617 Glu-90, F2-Glu-90 and F3-Glu-90), as compared to heated free-glucose films, being an
 618 indication of achievement of high interaction between chitosan and glucose due to thermal
 619 treatment, leading to the crosslinking through MR. Similarly, Etxabide et al. (2017) reported
 620 that a greater compact structure was observed for cross-sections of heated gelatin films with
 621 lactose, as compared to free-lactose films.



622



623



624 **Figure 5:** Surface and cross-section SEM micrographs of control chitosan (A), CDP-C1 (B)

625 and CDP-C2 (C) based films with and without glucose and heated films containing glucose.

626 3.8. Antioxidant activity of CDP-based MR crosslinked films

627 Preventing oxidative damage in foods is known as a critical function of packaging to meet
628 the challenge of preserving the quality of food products. Accordingly, antioxidant active
629 packaging is emerging as a promising material to satisfy the demands. With the applications of
630 antioxidant agents in food packaging materials, oxidation reactions are significantly reduced
631 and thereafter the shelf-life of food products is considerably prolonged.

632 The antioxidant potential of chitosan and CDP-based MR-treated films was investigated
633 through different *in vitro* antioxidant tests, including the free radical scavenging activity, using
634 DPPH and ABTS⁺ radicals, the reducing power and the total antioxidant activity (**Table 5**).

635 Results in the present work reveal that for all antioxidant tests investigated, values were
636 significantly ($p < 0.05$) higher in the heated-CDP-based MR crosslinked films (F1-Glu-90, F1-
637 Glu-90, F1-Glu-90) than in the blank chitosan-based film.

638 The ABTS⁺ radical scavenging activity showed that, prior to heat treatment and MR
639 induction, chitosan film (F1) exhibited the lowest potential ($56.50 \pm 0.50\%$) followed by F2
640 ($77.37 \pm 1.33\%$) and F3 ($84.55 \pm 0.39\%$), which is correlated to the Mw of chitosan samples
641 (the half-inhibition concentrations (IC_{50}) values were 1.61, 0.89 and 0.7 mg/ml, respectively)
642 (Affes et al., 2020b). Additionally, when glucose was added to the control films, a slight
643 increase without significant difference was obtained. Furthermore, thermal treatment of free-
644 glucose films at 90 °C showed significant increase of the radical scavenging capacity. However,
645 this effect is negligible, as compared to those of the heated-glucose-containing films.
646 Interestingly, after thermal treatment of these latter films, a higher significant increase of
647 antioxidant activity especially in the films containing lower Mw-CDP (96.04 ± 0.81 and
648 100.00%, using C1 and C24, respectively) was observed. Similarly, Kchaou et al. (2019)
649 reported that ABTS radical scavenging activity of fish gelatin films conjugated with glucose
650 was significantly improved after heating at 90 °C.

651 Regarding DPPH radical scavenging capacity, results showed that CDP-based films F2
652 and especially F3 exhibited higher effect (61.90 ± 1.05 and $70.10 \pm 0.50\%$, respectively), as
653 compared to chitosan film (F1) ($50.92 \pm 0.31\%$). This variation is attributed to the enhanced
654 radical scavenging activity of chitosan-derivatives in comparison to the native chitosan, as
655 shown in our previous study (IC_{50} values were about 3.07, 2.78 and 1.75 mg/ml for Ch, C1 and
656 C24, respectively) (Affes et al., 2020b). Further, glucose addition increased slightly the DPPH
657 radical scavenging activity in three different Mw-chitosan unheated films. However, the
658 activity of the heat-treated films increased significantly in comparison with non-heated ones,
659 especially after glucose supplementation. Thus, the highest radical scavenging capacity, which
660 reached $99.65 \pm 0.35\%$, was reached for the films containing the lowest Mw-CDP (F3-Glu-90),
661 followed by F2-Glu-90 ($84.62 \pm 1.05\%$) and F1-Glu-90 ($99.65 \pm 0.35\%$). Results demonstrate
662 that MRPs generated in the heated glucose-films increased the capacity of the films to donate
663 hydrogen atom, allowing to stabilize the free radicals. In this context, the ability of heat-induced
664 MRP to scavenge DPPH radical has been previously reported (Kchaou et al., 2019; Li et al.,
665 2014; Maillard, Billaud, Chow, Ordonaud, & Nicolas, 2007).

666 In addition, the films capacity to covert Fe^{3+} into Fe^{2+} was investigated. This test measures
667 particularly the antioxidant ability of MRPs as their hydroxyl groups play a role in the reducing
668 activity through their redox potential of transferring electrons (Vhangani & Van Wyk, 2013).
669 Results depicted in **Table 5** revealed that glucose addition enhanced the films reducing power
670 capacity even without heating and this increase is dependent on the Mw of chitosan/CDP
671 sample. Indeed, the highest optical absorbance at 700 nm was obtained for glucose-heated films
672 F3-Glu-90 (1.78 ± 0.03), followed by F2-Glu-90 (1.37 ± 0.07) and F1-Glu-90 (1.02 ± 0.06). On
673 the contrary, control unheated films showed the lowest antioxidant potential. Similarly, Li et
674 al. (2014) found that low Mw-chitosan conjugated with maltose showed higher reducing

675 activity than high and medium Mw chitosan-maltose systems of MRP during treatment at 100
676 °C.

677 Subsequently, the total antioxidant activity of the films was further studied. Control films
678 showed the lowest antioxidant ability (66.57 ± 1.23 , 72.10 ± 1.30 and 87.20 ± 0.78 α -tocopherol
679 ($\mu\text{mol/ml}$) for F1 F2 and F3, respectively). On the other hand, glucose addition resulted in a
680 slight enhancement of the films antioxidant effect, while an interesting increase was observed
681 once after thermal treatment at 90 °C. Therefore, results suggest that MRPs could react with
682 Mo (VI) to convert it into more stable molecules, Mo (V) by donating electrons (Kchaou et al.,
683 2018).

684 From these results, the heat treatment and especially MR development may be considered
685 as useful methods to improve the antioxidant ability of chitosan and CDP-based films, allowing
686 to conclude that glucose-containing films, especially, F3-Glu-90, could be used as an active
687 packaging in order to protect foods against oxidation.

688 **Table 5:** ABTS⁺ and DPPH radicals-scavenging activities (%), reducing power (OD_{700 nm}) and
689 total antioxidant activity (α -tocopherol ($\mu\text{mol/ml}$)) values of chitosan or CDP-based films
690 conjugated or not with glucose and before and after thermal treatment at 90 °C.

Antioxidant	ABTS radical scavenging activity (%)	DPPH radical scavenging activity (%)	Reducing power (OD _{700 nm})	Total antioxidant activity (α -tocopherol ($\mu\text{mol/ml}$))
F1	$56.50 \pm 0.50^{\text{H}}$	$50.92 \pm 0.31^{\text{H}}$	$0.22 \pm 0.01^{\text{H}}$	$66.57 \pm 1.23^{\text{I}}$
F1-90	$61.00 \pm 1.65^{\text{G}}$	$58.41 \pm 0.50^{\text{G}}$	$0.62 \pm 0.01^{\text{DE}}$	$73.77 \pm 0.54^{\text{GH}}$
F1-Glu	$57.12 \pm 0.84^{\text{H}}$	$53.12 \pm 0.03^{\text{H}}$	$0.48 \pm 0.02^{\text{FG}}$	$72.27 \pm 067^{\text{H}}$
F1-Glu-90	$70.76 \pm 0.88^{\text{F}}$	$68.59 \pm 1.24^{\text{E}}$	$1.02 \pm 0.06^{\text{C}}$	$97.21 \pm 1.01^{\text{C}}$
F2	$77.37 \pm 1.33^{\text{E}}$	$61.90 \pm 1.05^{\text{F}}$	$0.37 \pm 0.03^{\text{G}}$	$72.10 \pm 1.30^{\text{H}}$
F2-90	$83.69 \pm 0.65^{\text{D}}$	$70.35 \pm 0.70^{\text{E}}$	$0.72 \pm 0.01^{\text{D}}$	$80.51 \pm 2.12^{\text{F}}$
F2-Glu	$79.54 \pm 1.03^{\text{E}}$	$64.22 \pm 0.81^{\text{F}}$	$0.55 \pm 0.05^{\text{EF}}$	$76.47 \pm 1.45^{\text{G}}$
F2-Glu-90	$96.04 \pm 0.81^{\text{B}}$	$84.62 \pm 1.05^{\text{B}}$	$1.37 \pm 0.07^{\text{B}}$	$122.18 \pm 0.48^{\text{B}}$
F3	$84.55 \pm 0.39^{\text{D}}$	$70.10 \pm 0.50^{\text{E}}$	$0.57 \pm 0.02^{\text{EF}}$	$87.20 \pm 0.78^{\text{E}}$
F3-90	$92.35 \pm 0.84^{\text{C}}$	$81.34 \pm 73.80^{\text{C}}$	$0.92 \pm 0.01^{\text{C}}$	$95.50 \pm 0.56^{\text{CD}}$

F3-Glu	85.82 ± 0.61 ^D	73.80 ± 0.81 ^D	0.71 ± 0.05 ^D	92.24 ± 0.79 ^D
F3-Glu-90	100.00 ± 0.00 ^A	99.65 ± 0.35 ^A	1.78 ± 0.03 ^A	147.40 ± 0.91 ^A

691 Values are means ± standard deviation (n = 3). Means with different letters (A-I) and within a
692 column indicate significant difference ($p < 0.05$).

693 **4. Conclusion**

694 In this study, different Mw chitosan or chitosan depolymerisation products (CDP)-based
695 films, conjugated or not with glucose, were prepared and thermally treated at 90 °C during 24
696 h. Films physicochemical properties were enhanced by crosslinking through heat treatment, as
697 compared to unheated films, especially in the films containing glucose due to Maillard reaction
698 (MR) development. Meanwhile, the most efficient rate of MR was obtained by lower Mw-CDP
699 films as confirmed by higher color changes from transparent to brown and better light barrier
700 properties. However, water resistance properties, thermal stability and mechanical behavior
701 were found to be better in higher Mw chitosan based films. Furthermore, antioxidant potential
702 of heated films assessed by four different mechanisms proved that low Mw-CDP based films
703 and more precisely, crosslinked films through MR, showed strong antioxidant activities due to
704 the reinforcement of more functional active groups. The obtained results promote to control the
705 extension of crosslinking in order to select the appropriate conditions for each specific
706 application. It can be concluded that MR development is a viable method that leads to generate
707 bioactive compounds, which confer better functional and biological properties to chitosan and
708 CDP-based films to be satisfactory for food applications, as potential packaging that ensure
709 food safety and extend the shelf-life of packaged food.

710 **Credit authorship contribution statement**

711 **Sawsan Affes:** Conceptualization, Methodology, Validation, Formal analysis, Investigation,
712 Writing - Original Draft.

713 **Hana Maalej:** Supervision, Conceptualization, Resources, Writing - Review & Editing.

714 **Suming Li:** Project administration, Investigation.

715 **Rim Nasri:** Project administration, Investigation.

716 **Moncef Nasri:** Supervision, Resources, Visualisation, Writing - Review & Editing.

717 **Acknowledgements**

718 The “Ministry of Higher Education and Scientific Research”, Tunisia, funded this work.

719 The authors gratefully acknowledge financial support provided from the framework of PHC-

720 Utique program financed by CMCU project , grant N°: 19G0815.

721 **Declaration of Competing Interest**

722 The authors declare that there are no conflicts of interest.

723 **References**

724 Affes, S., Aranaz, I., Hamdi, M., Acosta, N., Ghorbel-Bellaaj, O., Heras, Á., Nasri, M., &

725 Maalej, H. (2019). Preparation of a crude chitosanase from blue crab viscera as well as its

726 application in the production of biologically active chito-oligosaccharides from shrimp

727 shells chitosan. *International Journal of Biological Macromolecules*, 139, 558 1–569.

728 Affes, S., Maalej, H., Aranaz, I., Acosta, N., Kchaou, H., Heras, Á., & Nasri, M. (2020a).

729 Controlled size green synthesis of bioactive silver nanoparticles assisted by chitosan and

730 its derivatives and their application in biofilm preparation. *Carbohydrate Polymers*, 236,

731 116063.

732 Affes, S., Maalej, H., Aranaz, I., Acosta, N., Heras, Á., & Nasri, M. (2020b). Enzymatic

733 production of low-*Mw* chitosan-derivatives: Characterization and biological activities

734 evaluation. *International Journal of Biological Macromolecules*, 144, 279–288.

735 Aljbour, N. D., Beg, M. D. H., & Gimbun, J. (2019). Acid hydrolysis of chitosan to oligomers
736 using hydrochloric acid. *Chemical Engineering & Technology*, *42*, 1741–1746.

737 Bersuder, P., Hole, M., & Smith, G. (1998). Antioxidants from a heated histidine-glucose model
738 system. I: Investigation of the antioxidant role of histidine and isolation of antioxidants by
739 high-performance liquid chromatography. *Journal of the American Oil Chemists' Society*,
740 *75*, 181–187.

741 Bharathidasan, T., Narayanan, T. N., Sathyanaryanan, S., & Sreejakumari, S. S. (2015). Above
742 170° water contact angle and oleophobicity of fluorinated graphene oxide based transparent
743 polymeric films. *Carbon*, *84*, 207–213.

744 De Britto, D., & Assis, O.B.G. (2007). A novel method for obtaining a quaternary salt of
745 chitosan. *Carbohydrate Polymers*, *69*, 305–310.

746 Etxabide, A., Urdanpilleta, M., Gómez-Arriaran, I., de la Caba, K., & Guerrero, P. (2017).
747 Effect of pH and lactose on cross-linking extension and structure of fish gelatin films.
748 *Reactive and Functional Polymers*, *117*, 140–146.

749 Etxabide, A., Urdanpilleta, M., Guerrero, P., & de la Caba., K. (2015). Effects of cross-linking
750 in nanostructure and physicochemical properties of fish gelatins for bio-application.
751 *Reactive and Functional Polymers*, *94*, 55–62.

752 Fernández-de Castro, L., Mengíbar, M., Sánchez, A., Arroyo, L., Villarán, M. C., de Apodaca,
753 E. D., & Heras, Á. (2016). Films of chitosan and chitosan-oligosaccharide neutralized and
754 thermally treated: Effects on its antibacterial and other activities. *LWT - Food Science and*
755 *Technology*, *73*, 368–374.

756 Gennadios, A., Handa, A., Froning, G. W., Weller, C. L., & Hanna, M. A. (1998). Physical
757 properties of egg white-dialdehyde starch films. *Journal of Agricultural and Food*
758 *Chemistry*, *46*, 1297–1302.

759 Gullón, B., Montenegro, M. I., Ruiz-Matute, A. I., Cardelle-Cobas, A., Corzo, N., & Pintado,
760 M. E. (2016). Synthesis, optimization and structural characterization of a chitosan-glucose
761 derivative obtained by the Maillard reaction. *Carbohydrate Polymers*, *137*, 382–389.

762 Hajji, S., Younes, I., Affes, S., Boufi, S., & Nasri, M. (2018). Optimization of the formulation
763 of chitosan edible coatings supplemented with carotenoproteins and their use for extending
764 strawberries postharvest life. *Food Hydrocolloids*, *83*, 375–392.

765 Hazaveh, P., Mohammadi Nafchi, A., & Abbaspour, H. (2015). The effects of sugars on
766 moisture sorption isotherm and functional properties of cold water fish gelatin films.
767 *International Journal of Biological Macromolecules*, *79*, 370–376.

768 Hosseini, M. H., Razavi, S. H., & Mousavi, M. A. (2009). Antimicrobial, physical and
769 mechanical properties of chitosan-based films incorporated with thyme, clove and
770 cinnamon essential oils. *Journal of Food Processing and Preservation*, *33*, 727–743.

771 Kchaou, H., Benbettaieb, N., Jridi, M., Nasri, M., & Debeaufort, F. (2019). Influence of
772 Maillard reaction and temperature on functional, structure and bioactive properties of fish
773 gelatin films. *Food Hydrocolloids*, *97*, 105196.

774 Kchaou, H., Benbettaieb, N., Jridi, M., Abdelhedi, O., Karbowskiak, T., Brachais, C. H., Léonard,
775 M. L., Debeaufort, F., & Nasri, M. (2018). Enhancement of structural, functional and
776 antioxidant properties of fish gelatin films using Maillard reactions. *Food Hydrocolloids*,
777 *83*, 326–339.

778 Kosaraju, S. L., Weerakkody, R., & Augustin, M. A. (2010). Chitosan-glucose conjugates:
779 Influence of extent of Maillard reaction on antioxidant properties. *Journal of Agricultural
780 and Food Chemistry*, *58*, 12449–12455.

781 Leceta, I., Guerrero, P., & de la Caba, K. (2013a). Functional properties of chitosan-based films.
782 *Carbohydrate Polymers*, *93*, 339–346.

783 Leceta, I., Guerrero, P., Ibarburu, I., Dueñas, M. T., & de la Caba, K. (2013b). Characterization
784 and antimicrobial analysis of chitosan-based films. *Journal of Food Engineering*, *116*,
785 889–899.

786 Li, S. L., Lin, J., & Chen, X.M. (2014). Effect of chitosan molecular weight on the functional
787 properties of chitosan-maltose Maillard reaction products and their application to fresh-
788 cut *Typha latifolia* L. *Carbohydrate Polymers*, *102*, 682–690.

789 Martins, J. T., Cerqueira, M. A., & Vicente, A. A. (2012). Influence of α -tocopherol on
790 physicochemical properties of chitosan-based films. *Food Hydrocolloids*, *27*, 220–227.

791 Matiacevich, S. B., & Pilar Buera, M. (2006). A critical evaluation of fluorescence as a potential
792 marker for the Maillard reaction. *Food Chemistry*, *95*, 423–430.

793 Maillard, M. N., Billaud, C., Chow, Y. N., Ordonaud, C., & Nicolas, J. (2007). Free radical
794 scavenging, inhibition of polyphenoloxidase activity and copper chelating properties of
795 model Maillard systems. *LWT-Food Science and Technology*, *40*, 1434–1444.

796 Park, H. J., Jung, S. T., Song, J. J., Kang, S. G., Vergano, P. J., & Testin, R. F. (1999).
797 Mechanical and barrier properties of chitosan-based biopolymer film. *Chitin and*
798 *Chitosan Research*, *5*, 19–26.

799 Prieto, P., Pineda, M., & Aguilar, M., (1999). Spectrophotometric quantitation of antioxidant
800 capacity through the formation of a phosphomolybdenum complex: Specific application
801 to the determination of Vitamin E. *Analytical Biochemistry*, *269*, 337–341.

802 Re, R., Pellegrini, N., Proteggente, A., Pannala, A., Yang, M., & Rice-Evans, C. (1999).
803 Antioxidant activity applying an improved ABTS radical cation decolorization assay.
804 *Free Radical Biology & Medicine*, *26*, 1231–1237.

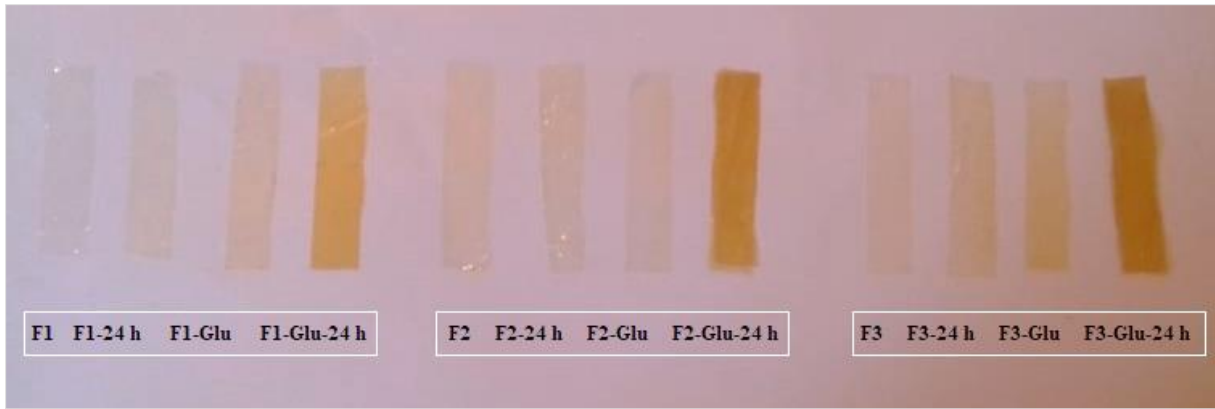
- 805 Rivero, S., Garía, M. A, & Pinotti, A. (2012). Heat treatment to modify the structural and
806 physical properties of chitosan-based films. *Journal of Agricultural and Food Chemistry*,
807 60, 492–499.
- 808 Ruban, S.W. (2009). Biobased packaging-application in meat industry. *Veterinary Word*, 2, 79–
809 82.
- 810 Sun, T., Qin, Y., Xu, H., Xie, J., Hu, D., Xue, B., & Hua, X. (2017). Antibacterial activities and
811 preservative effect of chitosan oligosaccharide Maillard reaction products on *Penaeus*
812 *vannamei*. *International Journal of Biological Macromolecules*, 105, 764–768.
- 813 Vhangani, L. N., & Van Wyk, J. (2013). Antioxidant activity of Maillard reaction products
814 (MRPs) derived from fructose-lysine and ribose-lysine model systems. *Food Chemistry*,
815 137, 92–98.
- 816 Yang, H., Li, J. G., Wu, N. F., Fan, M. M., Shen, X. L., Chen, M. T., Jiang, A. M., & Lai, L. S.
817 (2015). Effect of hsian-tsao gum (HG) content upon rheological properties of film-
818 forming solutions (FFS) and physical properties of soy protein/hsian-tsao gum films.
819 *Food Hydrocolloids*, 50, 211–218.
- 820 Yildirim, A., Mavi, A., & Kara, A.A. (2001). Determination of antioxidant and antimicrobial
821 activities of *Rumex crispus* L. extracts. *Journal of Agricultural and Food Chemistry*, 49,
822 4083–4089.

823

824

825

826 **Supplementary data**



827

828 **Figure S1:** Color change of chitosan and CDP based films with and without glucose (5%)
 829 addition and before and after heating process during 24 h at 90 °C.

830

831

832

833

834

835

836

837

838

839

840

841

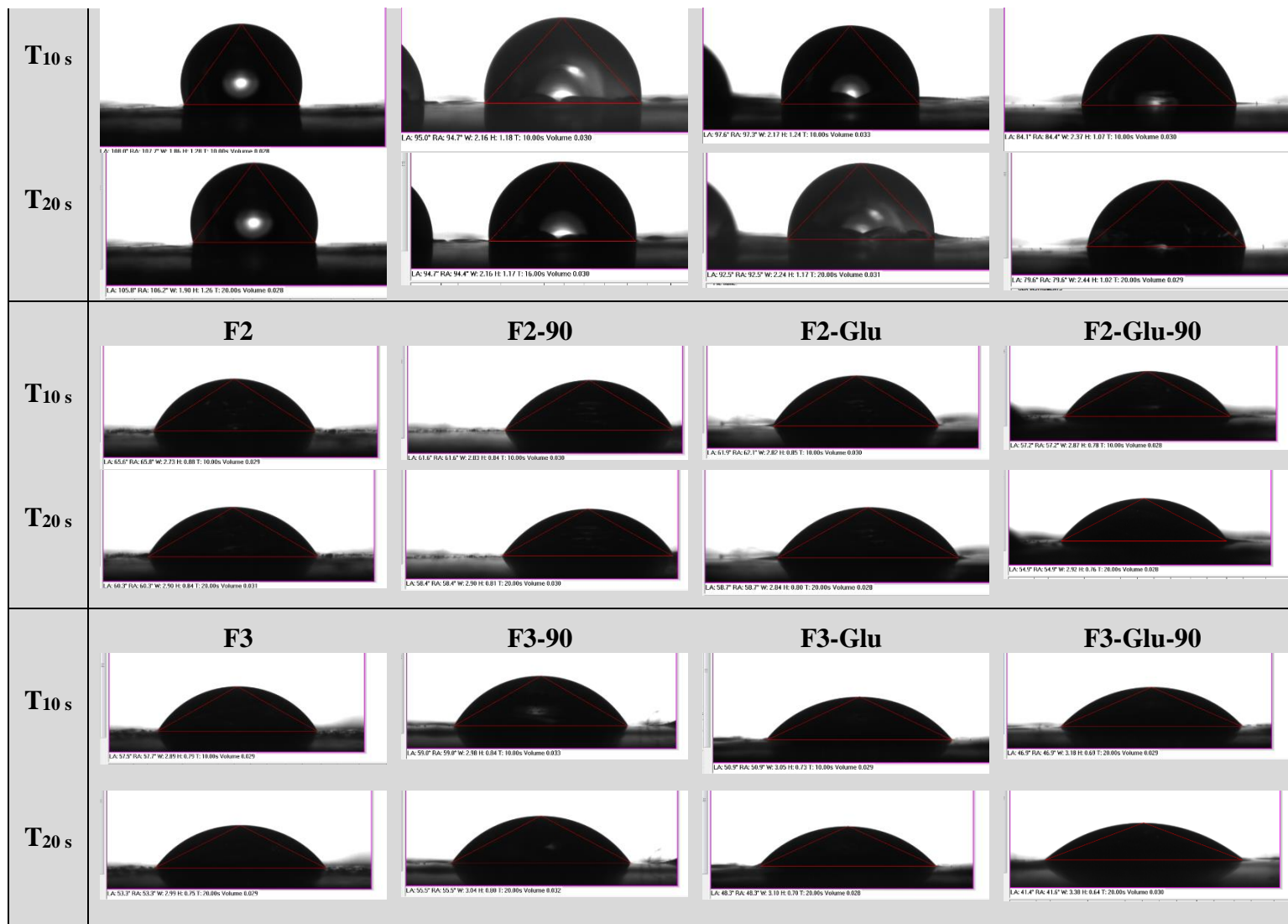
842

F1

F1-90

F1-Glu

F1-Glu-90



843 **Figure S2:** Shape and behavior of water droplets deposited on the surface of chitosan and CDP
844 films conjugated or not with glucose and before and after thermal treatment, as a function of
845 time (T = 10 and T = 20 s).